Corrigendum

The effects of fasting and cold exposure on metabolic rate and mitochondrial proton leak in liver and skeletal muscle of an amphibian, the cane toad *Bufo marinus*

M. Trzcionka, K. W. Withers, M. Klingenspor and M. Jastroch

There was an error published in *J. Exp. Biol.* **211**, 1911-1918.

In Fig. 4A, the symbols representing 'Liver fasted' and 'Liver fed' were transposed in the in-figure key. The black circles actually represent 'Liver fed', and the grey circles represent 'Liver fasted' (as stated in the figure caption and the text of the article). This error does not affect any of the conclusions of the article.

The authors apologise to readers for any inconvenience this may have caused.

The effects of fasting and cold exposure on metabolic rate and mitochondrial proton leak in liver and skeletal muscle of an amphibian, the cane toad *Bufo marinus*

M. Trzcionka[1,*], K. W. Withers[2], M. Klingenspor[1] and M. Jastroch[1]

[1]Department of Animal Physiology, Faculty of Biology, Philipps-Universität Marburg, Karl-von-Frisch-Strasse 8, 35043 Marburg, Germany and [2]Centre for Systems Biology, University of Southern Queensland, Toowoomba, Queensland, Australia

*Author for correspondence (e-mail: trzcionk@students.uni-marburg.de)

SUMMARY

Futile cycling of protons across the mitochondrial inner membrane contributes significantly to standard metabolic rate in a variety of ectothermic and endothermic animals, but adaptations of the mitochondrial bioenergetics to different environmental conditions have rarely been studied in ectotherms. Changes in ambient temperature and nutritional status have a great effect on the physiological demands of ectothermic amphibians and may require the adjustment of mitochondrial efficiency. In order to investigate the effect of temperature and nutritional status on the mitochondrial level, we exposed male cane toads to either 10°C or 30°C and fasted half of the animals in each group. Cold exposure resulted in a fourfold reduction of the resting metabolic rate whereas nutritional status had only minor effects. The mitochondrial adjustments to each condition were observed by comparing the proton leak kinetics of isolated liver and skeletal muscle mitochondria at 25°C. In response to cold exposure, liver mitochondria showed a decrease in proton conductance while skeletal muscle mitochondria were unchanged. Additional food deprivation had minor effects in skeletal muscle, but in liver we uncovered surprising differences in energy saving mechanisms between the acclimation temperatures: in warm-acclimated toads, fasting resulted in a decrease of the proton conductance whereas in cold-acclimated toads, the activity of the respiratory chain was reduced. To investigate the molecular mechanism underlying mitochondrial proton leakage, we determined the adenine-nucleotide transporter (ANT) content, which explained tissue-specific differences in the basal proton leak, but neither the ANT nor uncoupling protein (UCP) gene expression correlated with alterations of the proton leak in response to physiological stimuli.

Supplementary material available online at http://jeb.biologists.org/cgi/content/full/211/12/1911/DC1

INTRODUCTION

In contrast to a high and constant metabolic rate in endothermic mammals, the metabolism of ectothermic vertebrates is rather low. A study comparing the metabolism of an ectothermic desert lizard to an endothermic rodent at the same ambient temperature observed a sevenfold lower resting metabolic rate (RMR) of the ectotherm (Brand et al., 1991). The metabolic rate of ectotherms varies with environmental temperature and is extremely reduced at low ambient temperatures. For example, the amphibian *Rana temporaria* hibernates in ice-covered ponds and is exposed to cold temperatures ranging from 0.5 to 4°C (Bradford, 1983), limited food intake and low oxygen supply. In the cold, the metabolic rate of the frog is decreased up to 50% (Boutilier et al., 1997), which could be further decreased up to 75% in anoxic conditions (Donohoe and Boutilier, 1998). Under these harsh conditions, a high metabolic depression was required that prevented the depletion of body substrate stores by two- to threefold.

At the cellular level, the metabolic rate of frog myocytes and of turtle hepatocytes exposed to short-term anoxia fell to 20% of normoxic conditions (Buck et al., 1993; West and Boutilier, 1998). This metabolic depression in ectotherms can be achieved by decreasing ATP-consuming processes such as protein synthesis and ionic balance, and by increasing the efficiency of the energy producing pathways (Hochachka, 1986). Some ectothermic vertebrates are able to reallocate ATP demands between essential and non-essential

processes. In the freshwater turtle, anoxia leads to a decrease in protein synthesis, increasing the energetic proportion of the cellular ionic balance mediated by the Na^+-K^+-ATPase (Buttgereit, 1995).

The metabolic adjustments in cells from ectotherms are highly reflected at the mitochondrial level. Mitochodria are in the very centre of conversion from substrate energy to cellular energy (in the form of ATP). Changes in mitochondrial efficiency allow an organism to respond to different physiological conditions. The proton motive force generated by the respiratory chain is not fully used to drive the ATP synthase as protons also leak back to the matrix without the generation of ATP. Mitochondrial proton leakage contributes significantly (about 20%) to standard metabolic rate in endothermic (Brand et al., 1994; Porter and Brand, 1995; Rolfe et al., 1999) and ectothermic vertebrates (Brand et al., 1991; Bishop and Brand, 2000).

Isolated skeletal muscle mitochondria of frogs submerged in anoxic cold water showed a decreased phosphorylating (state 3) and a decreased leak (state 4) respiration (Boutilier and St-Pierre, 2002). In these frogs, a decreased leak was not achieved by a lowered proton conductance but by a reduction in the electron transport chain activity (Boutilier and St-Pierre, 2002). Similar results were obtained in the aestivating snail *Helix aspersa* (Bishop and Brand, 2000). Adjustments of mitochondrial proton leakage seem to be a general strategy to adapt an organism to changes in metabolic rate. Even in endothermic mammals, temporary hypometabolic states such as daily

torpor and hibernation require modulations of the mitochondrial oxidative phosphorylation in selected organs. Liver mitochondria of hibernating ground squirrels showed a decreased respiration and displayed a lowered membrane potential while no difference was found in skeletal muscle mitochondria (Barger et al., 2003). Notably, the decreased proton leak in liver mitochondria was achieved by lowering the activity of the respiratory chain and not *via* a decreased proton conductance of the mitochondrial inner membrane. Similar effects on the mitochondrial respiration were reported in liver mitochondria of daily heterotherms such as the Djungarian hamster (Brown et al., 2007).

The molecular nature of the mitochondrial proton leak and its regulation is not fully understood. Protons can either cross the phospholipid bilayer directly, or they are transported back into the mitochondrial matrix by membrane-integrated transport proteins. The direct proton leak through the phospholipid bilayer accounts for only 5% of the total proton leak (Brookes et al., 1997). Therefore, specific proteins in the mitochondrial inner membrane contribute primarily to proton leakage. Two groups of mitochondrial carrier proteins have been reported to contribute significantly to the proton leak: the adenine nucleotide translocator (ANT) and uncoupling proteins (UCPs).

The basal proton leak is significantly affected by the presence of the ANT, independent of its ATP/ADP-exchange function. Studies on skeletal muscle mitochondria in ANT1-ablated mice and in fruit flies expressing different amounts of ANT suggested that the ANT causes about 50% of the basal proton leak (Brand et al., 2005).

Inducible proton leak can be provoked by activators of the ANT and UCPs. Mammalian UCP1 in brown adipose tissue uncouples the mitochondrial respiration and dissipates the proton motive force as heat when activated with free fatty acids. The uncoupling function of all mammalian UCPs and the ANT can be induced by superoxides and intermediate products of lipid peroxidation to prevent their *de novo* production.

Recently, orthologous proteins of all three mammalian UCPs have been identified in ectothermic vertebrates (Jastroch et al., 2005) and an inducible uncoupling function in liver mitochondria coincides with high levels of carp UCP1 (Jastroch et al., 2007). Whether UCPs other than UCP1 affect the basal proton leak in ectotherms and elucidation of their physiological role, requires further studies.

Taken together, the regulation and molecular mechanisms of the mitochondrial proton leak in ectothermic vertebrates is not understood but may increase our knowledge of how mitochondrial adjustments contribute to physiological adaptations.

In our approach, we aimed to characterize the interdependence of metabolic depression and mitochondrial adjustments in an ectothermic vertebrate. Therefore, we investigated the effects of ambient temperature and fasting on metabolic rate and mitochondrial bioenergetics in the cane toad *Bufo marinus*. This species is indigenous to northern South America, where temperatures range from 7°C to 40°C throughout the whole year. In its natural habitat (subtropical forests close to freshwater) *Bufo marinus* feeds on almost every terrestrial animal (Hinckley, 1963), but also experiences food shortage and temperature variations, making it an appropriate organism for this study.

MATERIALS AND METHODS
Animal experiments

Adult male *Bufo marinus* Linnaeus 1758 (44 individuals, approximate body mass 100 g each) were obtained from a local supplier (Peter Douche, Mareeba, Queensland, Australia) and housed in the animal facility of the University of Southern Queensland, Toowoomba, Queensland, Australia. All cane toads were kept at 22°C for 7 days and force-fed daily with 1.0±0.1 g cat food (KiteKat, chicken) which is equivalent to 1±0.1% of body mass. After 7 days, one group of toads (16 individuals) was acclimated to 10°C (cold-acclimated; CA) in a constant temperature chamber and the other group (18 individuals) was acclimated to 30°C (warm-acclimated; WA) in an air-conditioned room for 9 days. Half of the cane toads in each temperature group were fed daily, while the other half was fasted. All animals were held on a 12 h:12 h light:dark cycle (12:12 L:D). Cane toads acclimated to 10°C were bathed in rainwater for 30 min, and toads acclimated to 30°C for 1 h each day, to prevent dehydration of the skin. Cane toads at 10°C had access to water for a shorter period to reduce the risk of drowning. A *Xenopus laevis* for the northern blot of multiple tissues was kindly provided by G. Schemken, Faculty of Medicine, Philipps-Universität Marburg. All animals were killed by double pithing. Experimental protocols for the use of the toads were approved by the Animal Ethics Committee of the University of Southern Queensland (permit no. 06REA299) and Environment Australia and were in accordance with the German Animal Welfare Laws.

Measurement of metabolic rate

The metabolic rate of each toad was determined at its acclimation temperature using an open flow system. Each toad was placed in a 0.5 l metabolic chamber inside a temperature controlled cabinet at T_a=10±0.5°C or 30±0.5°C without food or water. The rate of airflow was maintained at 65 ml min^{-1}. Metabolic rate was determined as the mean minimum relatively constant rate of oxygen consumption for three 10 min periods. Metabolic rate was determined using an Ametek S-3A/1 oxygen analyser and an FMA1812 mass flowmeter (Omega, Stamford, CT, USA) interfaced with an Osbourne FX16 computer by a PLC-814B modular DA & C card (Advantech, Milpita, CA, USA). A system of solenoid valves enabled the oxygen concentration of air from a calibration chamber to be measured, between measurements of air from the animal chamber. Rate of oxygen consumption was calculated using eqn 3a of Withers (Withers, 1977), assuming an RQ of 0.85. Animals were weighed before and after experiments and mean body mass used to calculate mass-specific metabolic rate.

Isolation of mitochondria

Mitochondria for proton conductance measurements were always isolated simultaneously from two cane toads from different experimental groups to minimize possible day-by-day variability in the quality of mitochondrial preparations. For skeletal-muscle mitochondria, the hind-leg skeletal muscle was finely diced in CP-1 medium (100 mmol l^{-1} KCl, 50 mmol l^{-1} Tris/HCl, pH 7.4, and 2 mmol l^{-1} EGTA), digested on ice for 10 min in CP-2 medium [CP-1, to which was added 0.5% (w/v) BSA, 5 mmol l^{-1} MgCl$_2$, 1 mmol l^{-1} ATP and 2.45 units ml^{-1} Protease Type VIII (Sigma P 5380)] and homogenized 15 times using a dounce homogenizer with a clearance of 0.2 mm between the glass tube and the pestle. The homogenate was transferred to a temperature-controlled centrifuge and spun at 500 *g* for 10 min at 4°C. The resulting supernatant was subjected to a high-speed spin cycle (10 600 *g*, 10 min, 4°C) and the resulting pellet was resuspended in CP-1. The high-speed spin cycle was repeated and the resuspension finally centrifuged at 3800 *g* for 10 min at 4°C. The final pellet was resuspended in a minimum volume of CP-1 buffer. For the isolation of liver mitochondria, the liver was removed, immediately placed in ice-cold isolation medium (250 mmol l^{-1} sucrose, 5 mmol l^{-1} Tris/HCl, pH 7.4, and 2 mmol l^{-1} EGTA), minced with scissors and disrupted eight times with the

dounce homogenizer. The homogenate was spun at $1000\,g$ for 3 min at 4°C, and the supernatant centrifuged at $10\,600\,g$ for 10 min, 4°C. The high-speed spin cycle was repeated twice and the final pellet resuspended in a minimal volume of isolation medium. The protein concentration of mitochondrial suspensions was determined by the biuret method using BSA as standard (Gornall et al., 1949).

Mitochondrial respiration

Oxygen consumption was measured using a Clarke-type electrode (Rank Brothers Ltd, Cambridge, UK) maintained at 25°C and calibrated with air-saturated medium [120 mmol l^{-1} KCl, 5 mmol l^{-1} K$_2$HPO$_4$, 3 mmol l^{-1} Hepes, 1 mmol l^{-1} EGTA, 0.3% (w/v) defatted BSA, 7 μmol l^{-1} rotenone (to inhibit complex I of the respiratory chain), adjusted to pH 7.2], which was assumed to contain 479 nmol O ml^{-1} (Reynafarje et al., 1985). Mitochondria were resuspended to a concentration of 3 mg protein ml^{-1} (liver) and 1.05 mg protein ml^{-1} (muscle) in the assay medium. Mitochondrial respiration was started by adding 4 mmol l^{-1} succinate. The respiratory control ratio (RCR), determined by dividing state 3 respiration by state 4 respiration, was measured once to ascertain the integrity of the mitochondria.

Proton leak kinetics

The kinetics of the mitochondrial proton leak was measured by determining the respiration rate required to drive the proton leak (measured in the presence of 1 μg ml^{-1} oligomycin). The mitochondrial membrane potential was measured simultaneously with mitochondrial respiration by using an electrode sensitive to the potential-sensitive probe, TPMP$^+$ (triphenylmethylphosphonium), in the presence of 150 nmol l^{-1} nigericin to dissipate the pH gradient, as described previously (Cadenas and Brand, 2000). The TPMP$^+$-sensitive electrode was calibrated with sequential additions of TPMP$^+$ up to 2.5 μmol l^{-1}, and succinate was added to initiate mitochondrial respiration. Membrane potential and respiration were progressively inhibited through successive steady states with the complex II inhibitor, malonate, up to 2 mmol l^{-1}. Finally FCCP (carbonyl cyanide p-trifluoromethoxyphenyl-hydrazone; 0.8 μmol l^{-1}) was added to dissipate the membrane potential and release all the TPMP$^+$ from the mitochondria, allowing correction for any small baseline drift. Respiration at each steady state was plotted against the corresponding membrane potential to verify the dependence of proton leak rate on the membrane potential.

Measurement of ANT content by CAT titre

CAT (carboxyatractylate) is a specific inhibitor of ANT, so the minimum amount of CAT required to lower state 3 respiration to the state 4 rate equals the amount of ANT present. To determine the CAT titre, excess ADP (300 μmol l^{-1}) was added to establish state 3, and then respiration was successively inhibited by small additions of CAT (0.5 μmol l^{-1} steps) until state 4 was well established. Respiration rate was plotted against CAT added and the minimum CAT titre was calculated as the intercept between the steepest slope and the state 4 rate (plus CAT). Results are presented as nmol CAT mg^{-1} protein; it is generally thought that one CAT molecule binds per ANT dimer (Streicher-Scott et al., 1993).

Comparative genomics

We conducted a comprehensive search for amphibian *UCP* genes by blasting the *Xenopus tropicalis* genome (Ensembl Genome Browser, http://www.ensembl.org) with full-length coding sequences of mammalian UCPs. As described previously (Jastroch et al., 2004), physical gene maps of verified *UCP* loci were scaled

based on assemblies of the Ensembl Genome Browser. Genes located up- and downstream of *UCP* genes in these loci were blasted against human, mouse and zebrafish genomes for the highest score.

RNA isolation and northern blot analysis

Total RNA was isolated using TRIzol (Gibco BRL), quantified and subjected to northern blot analysis as described previously (Jastroch et al., 2004). The membranes were hybridized using *Xenopus laevis* 251 bp UCP1 and 550 bp UCP2 cDNA probes derived with *Xenopus tropicalis* gene specific primers (UCP1: forward 5′-GGCTCCAGAGACAGATGAGCTTCGC-3′, reverse 5′-GGC-TATGGTTTTATAGGCGTCCATAGTGCC-3′; UCP2: forward 5′-GGTTCGGTTCCAAGCTCAGGCC-3′, reverse 5′-ATGGC-ACAGTTGATGGCGCTGG-3′).

Post-hybridization, the blots were washed with 2× SSC/0.1% SDS for 10 min, 1× SSC/0.1% SDS for 10 min, 0.5× SSC/0.1% SDS for 10 min and 0.1× SSC/0.1% SDS for 10 min at room temperature. Signal intensities were then monitored by exposure to a PhosphorScreen (Molecular Dynamics, Sunnyvale, CA, USA). The hybridized probes were then detected by phosphor imaging (Storm 860, Molecular Dynamics), and signal intensities were quantified using ArrayVision 7.0 (Imaging Research, St Catherines, ON, Canada). Ethidium bromide staining of total RNA served to normalize gel loading.

Statistical analysis

All values are reported as means ± standard error (s.e.m.). Statistical analysis was performed using Student's t-test for two group comparisons and two-way ANOVA (diet × acclimation temperature) for multiple group comparisons followed by Holm-Sidak *post-hoc* test. Results were considered statistically significant at $P<0.05$ (indicated with an asterisk).

RESULTS
Temperature effect on resting metabolic rate

The resting metabolic rates (RMR) of fed and fasted *B. marinus* were measured at their respective acclimation temperature. The mass-specific RMR in WA toads (fed: 0.083±0.008 ml O$_2$ g^{-1} h^{-1}; fasted: 0.078±0.008 ml O$_2$ g^{-1} h^{-1}) was about four times higher than in CA toads (fed: 0.019±0.001 ml O$_2$ g^{-1} h^{-1}; fasted: 0.018± 0.004 ml O$_2$ g^{-1} h^{-1}; $P<0.05$, Fig. 1). The body mass of the toads barely differed and therefore, a similar difference in whole animal metabolic rates was observed (see supplementary material Fig. S1). The nutritional status had minor effects on the metabolic rate but tended to be slightly lower in fasted cane toads. The RMR of WA toads was similar to that reported in other studies of *B. marinus* (0.081 ml O$_2$ g^{-1} h^{-1}) (Brookes et al., 1998), but lower than that in other amphibians such as the African clawed frog (0.279 ml O$_2$ g^{-1} h^{-1}) (Brookes et al., 1998), or reptiles such as the bearded dragon (0.109 ml O$_2$ g^{-1} h^{-1}) (Brand et al., 1991) or mammals such as the rat (0.779 ml O$_2$ g^{-1} h^{-1}) (Brand et al., 1991).

State 4 respiration and proton leak kinetics of liver and skeletal muscle mitochondria

We first compared the state 4 respiration rates measured at 25°C between liver and skeletal muscle mitochondria of all toads. Fig. 2 shows the respiration of liver and skeletal muscle mitochondria of WA fed toads as a representative result for all the other conditions. We found that skeletal muscle mitochondria displayed five times higher state 4 (leak) respiration rates than liver mitochondria (liver: 1.86±0.19 nmol O min^{-1} mg^{-1} protein; muscle: 9.64±1.06 nmol O min^{-1} mg^{-1} protein).
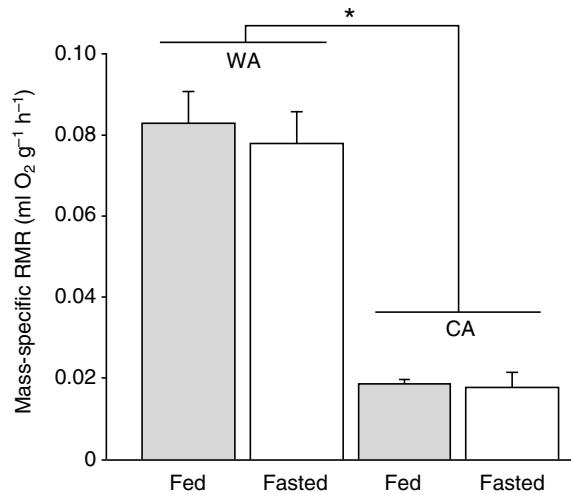
Fig. 1. Mass-specific resting metabolic rate (RMR; in ml O_2 g^{-1} h^{-1}) of fed and fasted cane toads acclimated to either 30°C (WA) or 10°C (CA), measured at their respective acclimation temperature. Values are means ± s.e.m., N=9 for warm acclimated and N=8 for cold acclimated toads. *P<0.05 (two-way ANOVA).
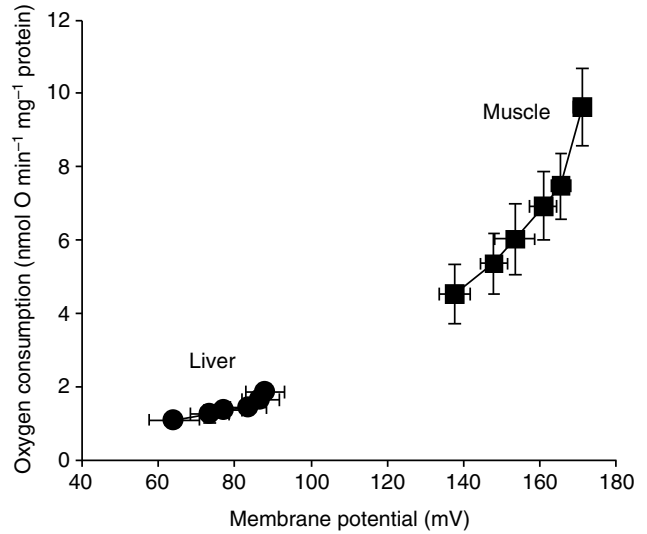

Fig. 2. Full kinetic response of the proton leak rate to changes in membrane potential of liver and skeletal muscle mitochondria of fed WA cane toads. Liver mitochondria have a lower basal proton leak than skeletal muscle mitochondria. A rough extrapolation of the skeletal muscle and the liver curve would suggest that the lower liver proton leak is achieved by a decrease in the respiratory chain activity and not *via* a change in the proton leak kinetic function. Values are means ± s.e.m., N=9.

We next compared the full kinetic response of the proton leak rate (measured as oxygen consumption) to changes in membrane potential of liver and skeletal muscle mitochondria of WA toads (Fig. 2). The proton leak of the toad mitochondria is a nonlinear function of membrane potential and the proton leak rate between two mitochondrial populations should usually be compared at a common membrane potential. In our leak titrations, the proton leak curves of liver and skeletal muscle mitochondria do not overlap, as a result of methodological restrictions. However, a rough extrapolation of the skeletal muscle and the liver curve would suggest that the lower liver proton leak is not achieved by a lower proton conductance but by a decrease in the respiratory chain activity.

Effect of cold acclimation on basal proton conductance of liver and skeletal muscle mitochondria

In liver mitochondria, cold acclimation did not change the state 4 respiration but increased the membrane potential significantly (WA:

88.025±5.07 mV; CA: 109.58±8.16 mV, P<0.05, Fig. 3A). This results in a shift of the proton leak curve to the right, which can be interpreted as a reduction of proton conductance in response to cold exposure. In contrast to the liver, cold exposure had no effect on the proton leak kinetics of skeletal muscle mitochondria (Fig. 3B).

The effect of food deprivation on proton conductance of liver and skeletal muscle

In liver mitochondria of WA toads, fasting shifted the proton leak curve to the right, without changing state 4 respiration (see supplementary material Fig. S2). Therefore, this decrease in the proton leak is achieved by a reduction of proton conductance while the respiratory chain activity is unaffected (fed state 4 potential: 88.025±5.07 mV, fasted state 4 potential: 123.39±3.67 mV, Fig. 4A).
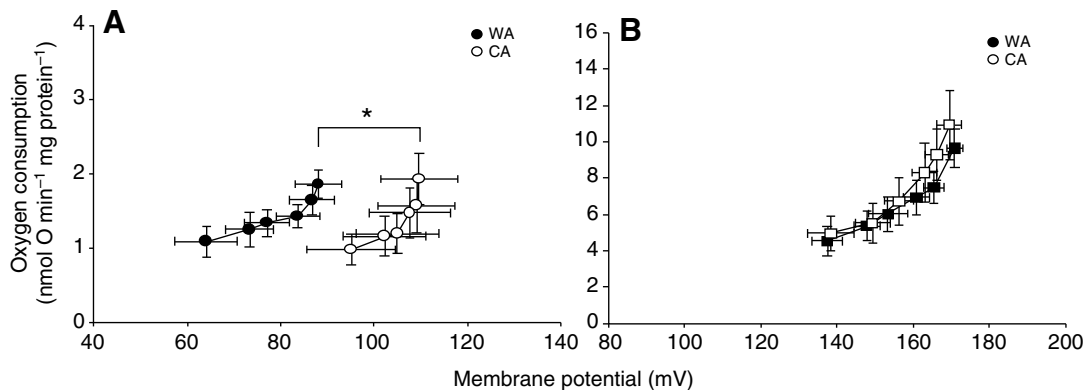

Fig. 3. Effect of acclimation temperature on proton leak kinetics of isolated liver (A) and skeletal muscle mitochondria (B) of fed cane toads. Experiments were carried out using liver mitochondria of CA (open circles) and WA (filled circles) and skeletal muscle mitochondria of CA (open squares) and WA (filled squares) cane toads. A shift of the proton leak curve to the right indicates a lower proton conductance of CA liver mitochondria (A), while the acclimation temperature has no effect in skeletal muscle mitochondria (B). Values are means ± s.e.m. from eight (CA group) or nine (WA group) independent preparations. *P<0.05 (two-way ANOVA).
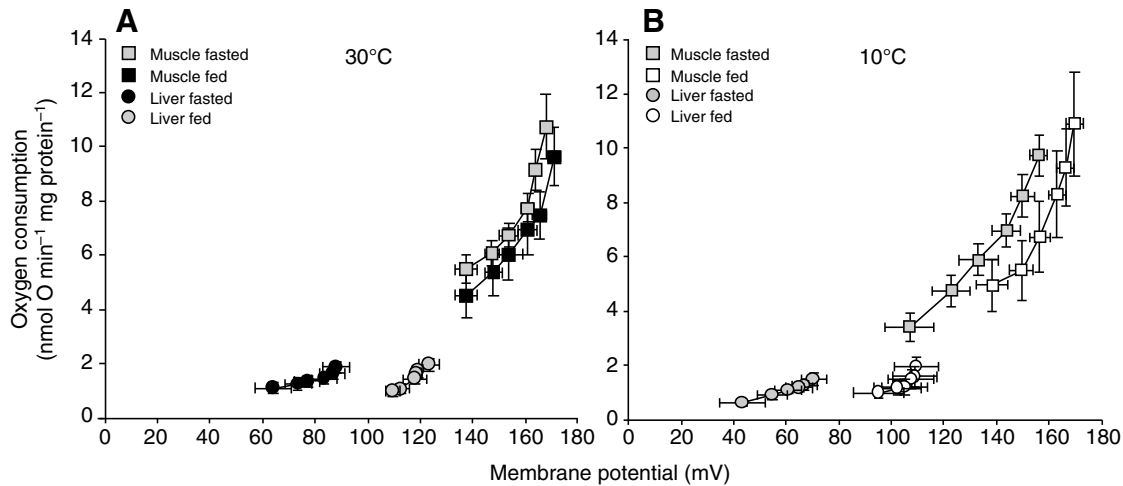
Fig. 4. Effect of fasting on proton leak kinetics of isolated liver and skeletal muscle mitochondria of WA (A) and CA (B) cane toads. Fasting revealed two different mechanisms of decreasing the proton leak in liver mitochondria (fasted toads, grey circles; WA fed toads, filled circles; CA fed toads, open circles), dependent on acclimation temperature. In WA toads (A), fasting caused a shift of the proton leak curve to the right, with no change in state 4 respiration but increased state 4 potential, thus suggesting a decrease in proton conductance (similar to Fig. 3; $P<0.05$ comparing state 4 membrane potential). In contrast, fasting in CA cane toads (B) resulted not only in a significant decrease of membrane potential ($P<0.05$) but also in a strong tendency towards lower state 4 respiration rates, suggesting a decreased respiratory chain activity. In skeletal muscle mitochondria, fasting has no effect on proton leakage at either acclimation temperatures (fasted toads, grey circles; WA fed toads, filled squares;, CA fed toads, open squares). Values are means ± s.e.m., N=8 for CA toads and N=9 for WA toads.

In contrast, fasting in the cold-acclimated toads shifted the curve to the left, but with a strong trend towards a decreased state 4 respiration (fed: 1.93±0.35 nmol O min^{-1} mg^{-1} protein, fasted: 1.47±0.23 nmol O min^{-1} mg^{-1} protein, see supplementary material Fig. S2). Furthermore, the membrane potential was significantly decreased in the fasted toads (fed: 109.58±8.16 mV; fasted: 70.35±4.78 mV, $P<0.05$, Fig. 4B). These results indicate that the decreased proton leak in fasted CA toads is achieved by a reduction of the respiratory chain activity or substrate oxidation.

In skeletal muscle mitochondria, fasting had only minor effects on the proton leak curves. The trend of the leak kinetics of the fasted CA toads was towards a higher proton conductance, but a lower state 4 respiration would suggest a lower basal leak during fasting in the cold.

Determination of the ANT content

To determine the molecular nature of the differences in the basal proton leak in different organs and under different physiological conditions, we investigated mitochondrial carrier proteins affecting the mitochondrial proton leak. It has been shown that the ANT catalyses up to two-thirds of the basal proton leak in insects and mammals (Brand et al., 2005). Therefore, we measured the ANT content in toad liver and skeletal muscle mitochondria by CAT
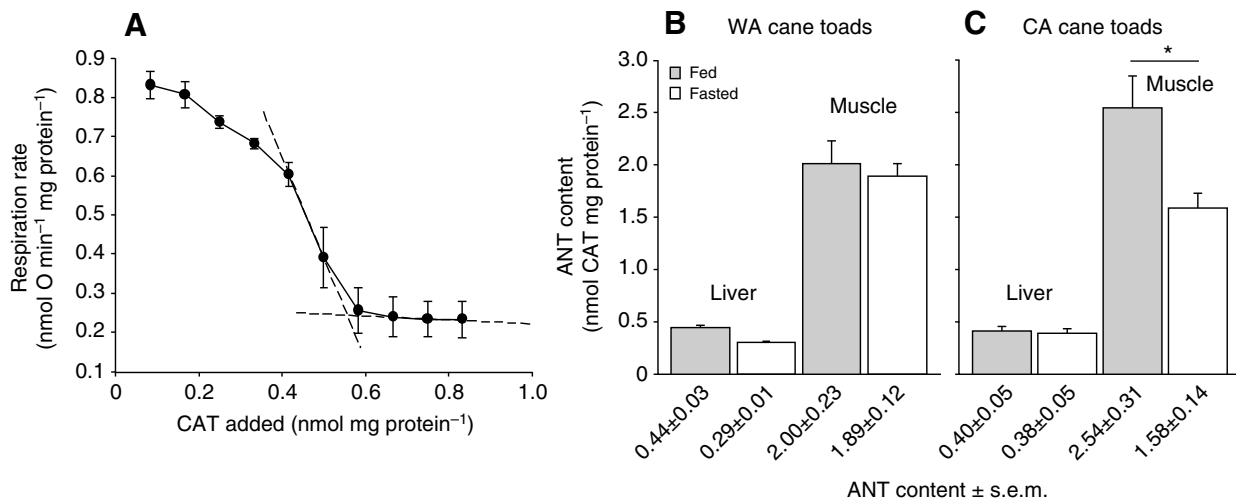

Fig. 5. Determination of the ANT content in isolated mitochondria by CAT titration. (A) CAT titre of respiration. State 3 respiration was titrated by successive additions of CAT to achieve state 4 respiration. ANT content was measured as the CAT titre where the steepest slope in the titration crosses the state 4 rate (broken lines). Results of a single representative determination are shown for liver mitochondria from fed cane toads acclimated to 30°C. (B,C) ANT contents of liver and skeletal muscle mitochondria of all experimental conditions measured by CAT titre (B, WA cane toads; C, CA cane toads). ANT content is about five times lower in liver mitochondria compared to skeletal muscle ($P<0.05$, two-way ANOVA.) but neither the temperature nor the nutritional status have an effect. Values are means ± s.e.m. from 4 independent preparations.*$P<0.05$ (two-way ANOVA).

titration (Fig. 5A). The titre of CAT needed to fully inhibit state 3 respiration rate to the state 4 rate was about fivefold greater in all skeletal muscle mitochondria as compared to liver ($P<0.05$, Fig. 5B,C). In liver mitochondria, the ANT content tended to be reduced by fasting in the WA toad (fed: 0.44±0.03; fasted: 0.29±0.01), while neither cold acclimation nor fasting in CA toads revealed a significant effect. In skeletal muscle mitochondria, a significant decrease in the ANT content was only found in response to fasting of CA toads (fed CA, 2.54±0.31 nmol CAT mg protein^{-1}; fasted CA, 1.58±0.14 nmol CAT mg protein^{-1}, $P<0.05$). We calculated that the ANT contributes to ~2.5% of total mitochondrial protein in liver mitochondria and ~13% in skeletal muscle. The ANT content of liver mitochondria from *B. marinus* (0.375±0.03 nmol CAT mg protein^{-1}) is in the same range of ANT concentration as found for mammalian liver. Mouse and rat liver mitochondria possess about 0.5 nmol CAT mg^{-1} protein^{-1} and larger mammals such as pigs and bovine both have lower ANT contents of about 0.25 nmol CAT mg^{-1} protein^{-1} (Brand et al., 2005). The ANT content of toad skeletal muscle mitochondria (1.99± 0.198 nmol CAT mg protein^{-1}) is also comparable to mammals (mice and rats: ~3 nmol CAT mg protein^{-1}; pigs 1.75 nmol CAT mg protein^{-1}) (Brand et al., 2005). Our results demonstrate that the ANT content of liver and skeletal muscle mitochondria is similar in endo- and ectotherms.

Characterization of UCPs in the cane toad

Besides the ANT, UCPs may also contribute to the proton leak but these proteins have to be activated, at least in mammals (Echtay, 2007). First, we identified a UCP1 and a UCP2/3 ortholog in the genome of the African clawed frog *Xenopus tropicalis* by conserved synteny, as described previously (see supplementary material Fig. S3) (Jastroch et al., 2005). Note that one of the neighbouring UCP2-UCP3 paralogous genes is extinguished in the amphibian lineage. Compared with their human orthologous proteins, frog UCP1 exhibits a similarity of 61% and frog UCP2/3 exhibits a similarity of 81% to human UCP2 and 69% to human UCP3. We cloned UCP1 and UCP2/3 cDNA fragments from *Xenopus laevis* liver and investigated the tissue-specific expression using northern blot analysis. While UCP1 mRNA levels were below detection levels of the northern blot analysis and could only be amplified using polymerase chain reaction, UCP2/3 mRNA was detected ubiquitously, with the highest amounts in intestine, spleen and kidneys (Fig. 6A). We then studied the regulation of UCP2/3 gene expression in liver and skeletal muscle of the cane toad. The northern blot signals were normalized and set to the value 1.0 for fed animals kept at 30°C, assuming that these conditions reflect their natural tropical habitat. In the liver, the acclimation of the toads to 10°C led to a significant sixfold increase of the UCP2/3 mRNA levels ($P<0.05$; Fig. 6B) while fasting had no effect. Cold exposure under fasted conditions, however, resulted in only 1.5-fold increase ($P<0.05$; Fig. 6B). In skeletal muscle, the UCP2/3 signals on the northern blot differed individually and did not show any pattern concerning regulation in response to acclimation temperatures and nutritional state (Fig. 6B).

DISCUSSION

In the present study, we demonstrate that the mitochondrial proton leak is highly regulated in response to ambient temperature and nutritional status in the ectothermic amphibian *B. marinus*, the cane toad. Our data strongly suggest that in periods of metabolic depression (low ambient temperature and food deprivation), mitochondrial efficiency in the toad is increased by lowering the proton leak in liver mitochondria to save energy. Cold exposure or food deprivation leads to a shift of the proton leak curve to the right, indicating a decrease in proton conductance of the mitochondrial inner membrane. Interestingly, within the CA animals, additional fasting shifts the curve to the left, suggesting a higher proton conductance. We observed, however, a reduction of state 4 respiration during fasting in the cold, indicating a decrease of the respiratory chain activity to lower the proton leak as has been previously observed in skeletal muscle mitochondria of hibernating frogs (Boutilier and St-Pierre, 2002).

We first showed that low ambient temperatures provoked a decrease of the resting metabolic rate in the ectothermic toad demonstrating that the metabolism is not maintained in the cold, as found for endotherms. Not surprisingly, metabolic rate dropped in the cold based on a Q10 of about 2. Although our toads were measured only at 30°C, their resting metabolic rate fell in the range measured for other ectotherms at 37°C and is comparable to values determined in other studies of the cane toad (Brand et al., 1991; Wang et al., 1995).

Mitochondria are the most important contributors to energy production and an adaption of mitochondrial efficiency may allow the animal to respond to physiological challenges. A strong correlation between metabolic rate and mitochondrial respiration and leak was reported previously (Brookes et al., 1998; Porter and Brand, 1993), and in the present study we investigated the effect of cold exposure and fasting on liver and skeletal muscle mitochondria in the cane toad. We found five times higher respiration rates in skeletal muscle mitochondria compared to liver mitochondria. This was expected, as among other vertebrates the aerobic capacity in muscle tissue is higher than in liver (Duong et al., 2006; Muleme et al., 2006). Although the liver and skeletal muscle leak curves do not overlap, a rough extrapolation suggests that the significantly lower basal proton leak in the liver is caused by a difference in the respiratory capacity. Cold exposure depressed the proton conductance in the liver while only minor effects were observed in skeletal muscle, suggesting other mechanisms of metabolic depression, such as reduced blood flow. In the liver, the decreased proton leak would result in a higher efficiency of energy conversion from nutrient to cellular energy. In amphibians, low ambient temperature leads to inactivity and reduces foraging (Paladino, 1985). Therefore, nutrient energy availability for the toad is greatly reduced, and a high mitochondrial efficiency would extend the depletion time of intrinsic body energy stores. The decrease of proton conductance seems to be a general energy saving mechanism, as similar effects were observed in lower vertebrates such as the cold-exposed common carp (Jastroch et al., 2007), and in higher vertebrates such as hibernating mammals (Barger et al., 2003). Similar to hibernating mammals, we found cold-depression on the mitochondrial proton leak in liver but not in skeletal muscle of the cane toad. Fasting of WA toads also had reducing effects on the liver mitochondrial proton leak by shifting the proton leak curve towards higher membrane potentials. Fasting of CA toads did not further shift the proton leak curve to the right, as would be expected when metabolic depression of cold and fasting were additive. Surprisingly, we observed a shift to the left, suggesting a higher proton leak. In contrast to other conditions, however, this shift of the curve was accompanied by a trend towards a reduced state 4 respiration, indicating a decrease in the respiratory chain activity. A strong reduction of the proton motive force (measured as membrane potential) can also be well interpreted as 'inactivity' of the mitochondrion as the driving force for mitochondrial metabolite exchange and energy turnover is minimized.
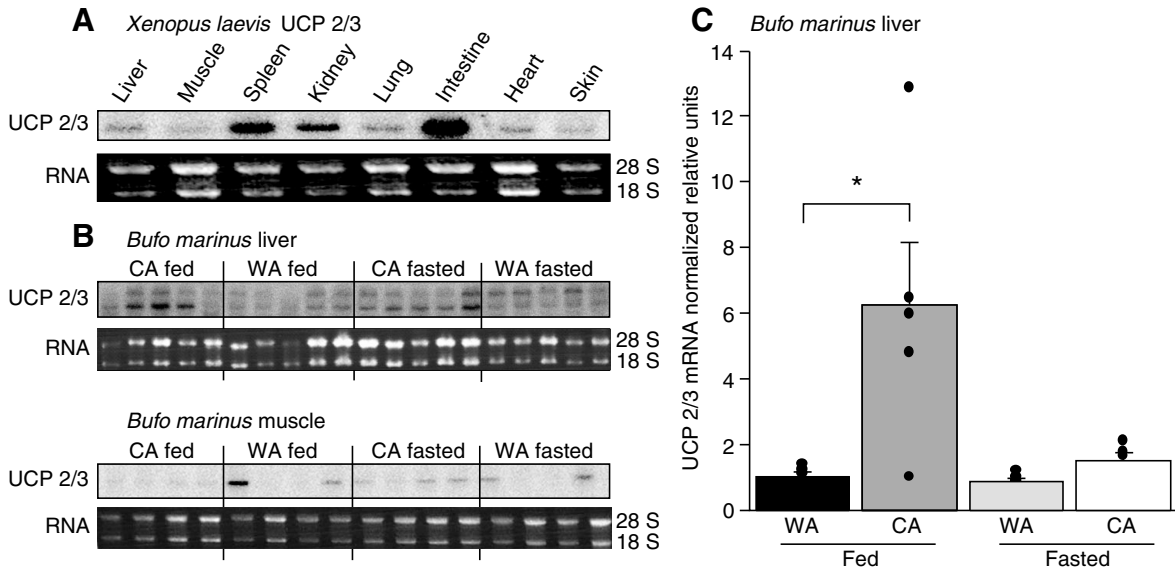
Fig. 6. Regulation of *UCP2/3* gene expression in amphibians in response to cold and food deprivation. 5 μg total RNA were hybridized with homologous *Xenopus laevis* UCP2/3 probes. (A) Northern blot analysis showing tissue-specific expression of UCP2/3 in *X. laevis*. (B) UCP2/3 mRNA expression levels in liver and skeletal muscle of *B. marinus* in response to cold and fasting. In the liver, cold caused a significant upregulation of UCP2/3 mRNA expression levels while fasting had no effect. In skeletal muscle, no effect of acclimation temperature and fasting was found due to high individual differences. (C) The scatter plot overlaying the bar charts shows the individual values for *B. marinus* liver. Values are means of four animals per group; *$P < 0.05$, two-way ANOVA.

Furthermore, the skeletal muscle proton leak kinetics of the fasted CA cane toad also pointed towards a reduction in respiratory chain activity, as state 4 respiration and membrane potential tended to be lower. In accordance with our results, a study on hibernating submerged frogs, also food-deprived and cold-acclimated for about 4 months, found a decrease of the skeletal muscle proton leak mainly caused by a reduction of the respiratory chain activity (Boutilier and St-Pierre, 2002).

However, a closer look at the proton leak kinetics in skeletal muscle exposed a slight increase in proton conductance in response to fasting. The additional proton leakage, apparent in liver and skeletal muscle of fasted CA toads, may serve to mildly uncouple the mitochondrial respiration and therefore reduce the oxidative stress by prevention of superoxide production. Previous studies demonstrate that oxidative stress may be dependent on substrate utilization and temperature (Muller et al., 2008; Farmer and Sohal, 1987). Further experimentation, including measurements of

mitochondrial superoxide production and substrate utilization, particularly on fed and fasted CA toads, is required to substantiate the surprising results in fasted CA toads.

Our results suggest that two strategies are used to decrease the mitochondrial proton leak in the liver of the cane toad: (i) changing the proton conductance (which results in a shift of the proton leak curve to the right), and (ii) lowering the activity of the electron transport chain, which may not change the proton leak kinetic function but results in a lower state 4 respiration and membrane potential (summarized in Fig. 7).

In order to investigate the molecular mechanism underlying changes in basal proton conductance, we determined the ANT content of isolated mitochodria by CAT titration. The ANT concentration explains the basal proton leak difference between liver and skeletal muscle where a four- to fivefold difference in ANT content reflects the four- to fivefold difference in respiration. Furthermore, the tendency towards a reduced ANT content in fasted
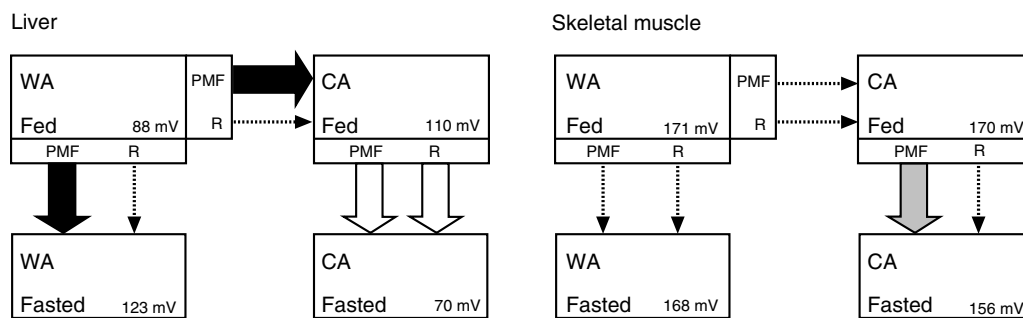

Fig. 7. Model summarizing mitochondrial bioenergetics in response to cold exposure and fasting. Effects on proton motive force (PMF, measured as membrane potential) and respiration (R, measured as state 4 respiration) in liver and skeletal muscle mitochondria. The boxes show the four conditions analyzed and include the state 4 membrane potentials (mV). Arrows indicate the changes in membrane potential and/or respiration in response to cold and/or fasting: black arrows, an increase; white arrows, a decrease; broken arrows, no change. In the liver, cold or fasting lead to an increase in membrane potential, while additional fasting in the cold causes an decrease in state 4 membrane potential and respiration rate. In skeletal muscle of cold-acclimated toads, fasting leads to a decrease in state 4 membrane potential.

WA toads is in accordance with a reduced basal proton conductance in response to fasting, but does not explain the adjustments of the proton leak observed during cold acclimation. Under these conditions, the molecular mechanism underlying adjustment of the proton leak is unknown and requires further investigation. Parameters of interest may be the ANT uncoupling activity and/or the membrane composition, which will also affect the basal proton leak (Shabalina et al., 2006; Brookes et al., 1998).

Some of the best-characterised proteins modulating the proton conductance in mitochondria are UCPs. In this study, we demonstrate the presence of UCP1 and a UCP2/UCP3 ortholog in amphibians. While UCP1 mRNA levels were barely detectable in liver and skeletal muscle, UCP2/3 mRNA was found by northern blot analysis. Most likely, amphibian UCP2/3 does not contribute to basal proton leak as cold acclimation increases mRNA levels, but lowers the proton leak. In fish and mammals, proton transport by UCP2 and UCP3 is attenuated and requires activators such as fatty acids, 4-hydroxynonenal and superoxides. It may well be that amphibian UCPs catalyse proton transport that may provide protection from reactive oxygen species by mild uncoupling, as predicted for mammalian UCP2 and UCP3 orthologs (Affourtit et al., 2007).

This study demonstrates the high plasticity of mitochondrial proton leakage in ectotherms exposed to physiological challenges such as cold exposure and food deprivation. Four possbie ways to change the proton leak have already been listed: (1) altering the proton leak kinetics, (2) changing the activity of the electron transport chain activity, (3) altering the volume density in cells, and (4) altering the cristae surface within the mitochondria (Boutilier and St-Pierre, 2002). In the cane toad, we observed two of these strategies, the alteration of the proton leak kinetics and the decrease of the respiratory chain activity. The molecular mechanism underlying these adjustments remains unknown and the presence of alternative strategies [listed as (3) and (4)] to alter the proton leak require further investigation.

LIST OF ABBREVIATIONS

ANT	adenine nucleotide translocator
CA	cold acclimated
CAT	carboxyatractylate
FCCP	carbonyl cyanide p-trifluoromethoxyphenylhydrazone
PMF	proton motive force
RCR	respiratory control ratio
RMR	resting metabolic rate
SMR	standard metabolic rate
T_a	ambient temperature
TPMP$^+$	triphenylmethylphosphonium
UCP	uncoupling protein
WA	warm acclimated

REFERENCES

Affourtit, C., Crichton, P. G., Parker, N. and Brand, M. D. (2007). Novel uncoupling proteins. *Novartis Found Symp.* **287**, 70-80, discussion 80-91.

Barger, J. L., Brand, M. D., Barnes, B. M. and Boyer, B. B. (2003). Tissue-specific depression of mitochondrial proton leak and substrate oxidation in hibernating arctic ground squirrels. *Am. J. Physiol.* **284**, R1306-R1313.

Bishop, T. and Brand, M. D. (2000). Processes contributing to metabolic depression in hepatopancreas cells from the snail *Helix aspersa*. *J. Exp. Biol.* **203**, 3603-3612.

Boutilier, R. G. and St-Pierre, J. (2002). Adaptive plasticity of skeletal muscle energetics in hibernating frogs: mitochondrial proton leak during metabolic depression. *J. Exp. Biol.* **205**, 2287-2296.

Boutilier, R. G., Donohoe, P. H., Tattersall, G. J. and West, T. G. (1997). Hypometabolic homeostasis in overwintering aquatic amphibians. *J. Exp. Biol.* **200**, 387-400.

Bradford, D. F. (1983). Winterkill, oxygen relations and energy metabolism of a submerged dormant amphibian, *Rana muscosa*. *Ecology* **64**, 1171-1183.

Brand, M. D., Couture, P., Else, P. L., Withers, K. W. and Hulbert, A. J. (1991). Evolution of energy metabolism. Proton permeability of the inner membrane of liver mitochondria is greater in a mammal than in a reptile. *Biochem. J.* **275**, 81-86.

Brand, M. D., Couture, P. and Hulbert, A. J. (1994). Liposomes from mammalian liver mitochondria are more polyunsaturated and leakier to protons than those from reptiles. *Comp. Biochem. Physiol.* **108B**, 181-188.

Brand, M. D., Pakay, J. L., Ocloo, A., Kokoszka, J., Wallace, D. C., Brookes, P. S. and Cornwall, E. J. (2005). The basal proton conductance of mitochondria depends on adenine nucleotide translocase content. *Biochem. J.* **392**, 353-362.

Brookes, P. S., Rolfe, D. F. and Brand, M. D. (1997). The proton permeability of liposomes made from mitochondrial inner membrane phospholipids: comparison with isolated mitochondria. *J. Membr. Biol.* **155**, 167-174.

Brookes, P., Buckingham, J., Tenreiro, A., Hulbert, A. and Brand, M. (1998). The proton permeability of the inner membrane of liver mitochondria from ectothermic and endothermic vertebrates and from obese rats: correlations with standard metabolic rate and phospholipid fatty acid composition. *Comp. Biochem. Physiol.* **119B**, 325-334.

Brown, J. C., Gerson, A. R. and Staples, J. F. (2007). Mitochondrial metabolism during daily torpor in the dwarf Siberian hamster: role of active regulated changes and passive thermal effects. *Am. J. Physiol.* **293**, R1833-R1845.

Buck, L. T., Hochachka, P. W., Schön, A. and Gnaiger, E. (1993). Microcalorimetric measurement of reversible metabolic suppression induced by anoxia in isolated hepatocytes. *Am. J. Physiol.* **265**, R1014-R1019.

Buttgereit, F. and Brand, M. D. (1995). A hierarchy of ATP-consuming processes in mammalian cells. *Biochem. J.* **312**, 163-167.

Cadenas, S. and Brand, M. D. (2000). Effects of magnesium and nucleotides on the proton conductance of rat skeletal-muscle mitochondria. *Biochem. J.* **348**, 209-213.

Donohoe, P. H. and Boutilier, R. G. (1998). The protective effects of metabolic rate depression in hypoxic cold submerged frogs. *Respir. Physiol.* **111**, 325-336.

Duong, C. A., Sepulveda, C. A., Graham, J. B. and Dickson, K. A. (2006). Mitochondrial proton leak rates in the slow, oxidative myotomal muscle and liver of the endothermic shortfin mako shark (*Isurus oxyrinchus*) and the ectothermic blue shark (*Prionace glauca*) and leopard shark (*Triakis semifasciata*). *J. Exp. Biol.* **209**, 2678-2685.

Echtay, K. S. (2007). Mitochondrial uncoupling proteins – what is their physiological role? *Free Radic. Biol. Med.* **43**, 1351-1371.

Farmer, K. J. and Sohal, R. S. (1987). Effects of ambient temperature on free radical generation, antioxidant defenses and life span in the adult housefly, *Musca domestica*. *Exp. Gerontol.* **22**, 59-65.

Gornall, A. G., Bardawill, C. J. and David, M. M. (1949). Determination of serum proteins by means of the biuret reaction. *J. Biol. Chem.* **177**, 751-766.

Hinckley, A. D. (1963). The diet of the giant toad, *Bufo marinus* (L.) in Fiji. *Herpetologica* **18**, 253-259.

Hochachka, P. W. (1986). Defense strategies against hypoxia and hypothermia. *Science* **231**, 234-241.

Jastroch, M., Withers, K. and Klingenspor, M. (2004). Uncoupling protein 2 and 3 in marsupials: identification, phylogeny, and gene expression in response to cold and fasting in *Antechinus flavipes*. *Physiol. Genomics* **17**, 130-139.

Jastroch, M., Wuertz, S., Kloas, W. and Klingenspor, M. (2005). Uncoupling protein 1 in fish uncovers an ancient evolutionary history of mammalian nonshivering thermogenesis. *Physiol. Genomics* **22**, 150-156.

Jastroch, M., Buckingham, J. A., Helwig, M., Klingenspor, M. and Brand, M. D. (2007). Functional characterisation of UCP1 in the common carp: uncoupling activity in liver mitochondria and cold-induced expression in the brain. *J. Comp. Physiol. B* **177**, 743-752.

Muleme, H. M., Walpole, A. C. and Staples, J. F. (2006). Mitochondrial metabolism in hibernation: metabolic suppression, temperature effects, and substrate preferences. *Physiol. Biochem. Zool.* **79**, 474-483.

Muller, F. L., Liu, Y., Abdul-Ghani, M. A., Lustgarten, M. S., Bhattacharya, A., Jang, Y. C. and Van Remmen, H. (2008). High rates of superoxide production in skeletal-muscle mitochondria respiring on both complex I- and complex II-linked substrates. *Biochem. J.* **409**, 491-499.

Paladino, F. V. (1985). Temperature effects on locomotion and activity bioenergetics of amphibians, reptiles and birds. *Am. Zool.* **25**, 965-972.

Porter, R. K. and Brand, M. D. (1993). Body mass dependence of H$^+$ leak in mitochondria and its relevance to metabolic rate. *Nature* **362**, 628-630.

Porter, R. K. and Brand, M. D. (1995). Causes of differences in respiration rate of hepatocytes from mammals of different body mass. *Am. J. Physiol.* **269**, R1213-R1224.

Reynafarje, B., Costa, L. E. and Lehninger, A. L. (1985). O$_2$ solubility in aqueous media determined by a kinetic method. *Anal. Biochem.* **145**, 406-418.

Rolfe, D. F. S., Newman, J. M. B., Buckingham, J. A., Clark, M. G. and Brand, M. D. (1999). Contribution of mitochondrial proton leak to respiration rate in working skeletal muscle and liver and to SMR. *Am. J. Physiol.* **276**, C692-C699.

Shabalina, I. G., Kramarova, T. V., Nedergaard, J. and Cannon, B. (2006). Carboxyatractyloside effects on brown-fat mitochondria imply that the adenine nucleotide translocator isoforms ANT1 and ANT2 may be responsible for basal and fatty-acid-induced uncoupling respectively. *Biochem. J.* **399**, 405-414.

Streicher-Scott, J., Lapidus, R. and Sokolove, P. M. (1993). Use of carboxyatractylate and tight-binding inhibitor theory to determine the concentration of functional mitochondrial adenine nucleotide translocators in a reconstituted system. *Anal. Biochem.* **210**, 69-76.

Wang, T., Burggren, W. and Nobrega, E. (1995). Metabolic, ventilatory, and acid-base responses associated with specific dynamic action in the toad *Bufo marinus*. *Physiol. Zool.* **68**, 192-205.

West, T. G. and Boutilier, R. G. (1998). Metabolic suppression in anoxic frog muscle. *J. Comp. Physiol. B* **168**, 273-280.

Withers, P. C. (1977). Measurement of V_{O_2}, V_{CO_2}, and evaporative water loss with a flow-through mask. *J. Appl. Physiol.* **42**, 120-123.